PORE SIZE DISTRIBUTION INDEX AND FALLING RATE STAGE OF EVAPORATION

Kyushu University Student Member ○Jumana Hussary
Kyushu University Regular Member Adel Alowaisy
Kyushu University Fellow Member Noriyuki Yasufuku
Kyushu University Regular Member Ryohei Ishikura

1. INTRODUCTION

Desertification is a serious environmental challenge of our century. Around 12 million hectares of land are lost yearly to droughts and desertification. Finding innovative solutions for this phenomenon is indispensable. One of the main factors that exacerbate the issue is the rising evaporation rates in drylands. Therefore, it is essential to accurately determine the evaporation rates from soil profiles. The evaporation process is divided into three stages that differ in their actual evaporation rate (AE) due to the change in the water transport mechanism within the profile. During the constant rate stage (Stage 1), water transports through liquid-filled pores from the drying front (the boundary between saturated and unsaturated layer) to the soil surface. The capillary transport maintains a high and constant AE during this stage. However, this hydraulic connection is disrupted at a specific drying front depth, and an air-dry layer is formed at the top of the profile. As a result, the water supply reduces, where water transports through capillary followed by vapor diffusion through the air-dry layer. Due to this change, a sharp drop in AE occurs, announcing the falling rate stage (Stage 2). AE recedes steadily until it converges to a low and constant value, marking the residual stage (Stage 3).

Stage 1 is relatively well understood in the literature. Yet, many questions are unanswered regarding Stage 2, and its complexity makes determining its AE challenging. Besides, previous research mentioned the significant role of Stage 2 in the process, especially in drylands (Hussary et al. 2022a). Many studies highlighted the complexity of studying the influence of soil properties on the process. However, a recent study by Hussary et al. (2022a) proposed a comprehensive and robust index that reflects the variation in the soil microstructure and correlates well with the evaporation process. The Pore Size Distribution Index (I_{PSD}) considers both water transport mechanisms involved in the process. Therefore, this present study focuses on the ability of the I_{PSD} in reflecting the efficiency of the soil profile to supply water which in turn controls the AE during Stage 2.

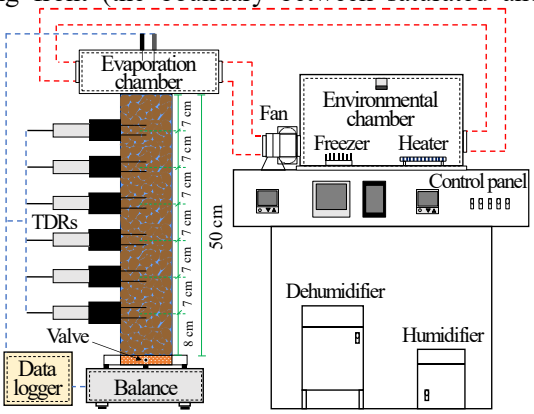

Figure 1: Experimental setup (Schematic)

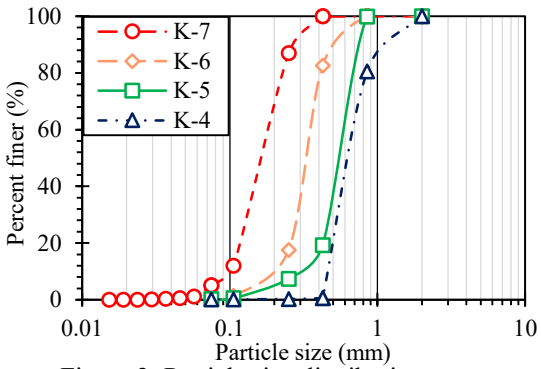

Figure 2: Particle size distribution curves

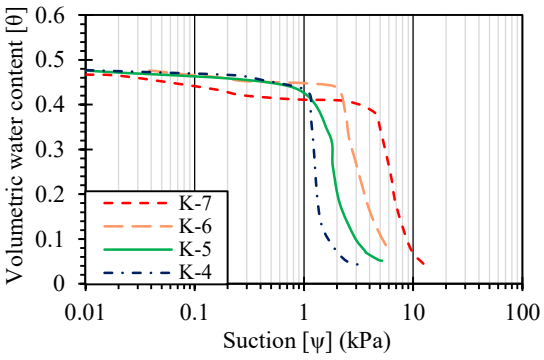

Figure 3: Soil water characteristic curves

2. MATERIALS AND METHODOLOGY

1-D homogeneous drying soil column tests were conducted. The experimental setup is shown in Figure 1. The columns were initially fully saturated to entirely capture the evaporation stages. The evaporation was allowed from the top through the evaporation chamber under constant atmospheric conditions. The temperature was maintained at 28.8±1.3℃, relative humidity at 48.2±4.5%, and wind speed at 2.2±0.2 m/s. The columns were mounted on a digital balance to determine the AE during testing. TDRs (moisture sensors) were attached along the column to trace the unsaturated layer development. The testing was stopped once Stage 3 began. For testing, four different textures of standard silica sand were used. The particle size distribution curves are shown in Figure 2. The columns were compacted at 80% relative density. A summary of the soil columns' physical properties is shown in Table 1. Figure 3 delineates the samples' Soil Water Characteristics Curves (SWCCs) determined

Keywords: Actual evaporation, Falling rate stage, Pore size distribution index, Unsaturated soil
Contact address: 744 Motooka, Nishi Ward, Fukuoka, 819-0395, Japan, Tel: +80-2-2999-7805

using the continuous pressurization method (Alowaisy et al., 2020). The Pore Size Distribution curves (PSD), shown in Figure 4, were inferred from the SWCCs, following Hussary et al. (2022a). The scatter plots delineate the calculated pore diameters while the smooth lines show their lognormal distribution fitting. The I_{PSD} was calculated as shown in Eq. (1) and Table 1:

$$I_{PSD} = \left(\frac{1}{d_1} - \frac{1}{d_2}\right) \times CV \quad (1)$$

where $(1/d_1)$-$(1/d_2)$ corresponds to the width of the PSD, which expresses the maximum capillary drive during drying. d_1 and d_2 are the smallest and largest capillaries in the sample, corresponding to the residual and air-entry suction values, respectively. While CV is the coefficient of variation of the fitted lognormal distribution representing the vapor diffusion zone.

3. RESULTS AND DISCUSSION

Figure 5 delineates the normalized actual evaporation curves of the tested soil columns. The normalized actual rate (Normalized AE) was found by dividing the AE during drying over the AE during Stage 1 (AE_i). It was noticed that the change in the AE during Stage 2 varied between the soil profiles. The normalized actual evaporation rate reduction slope during Stage 2 (ΔAE), indicated on each curve in Figure 5, was calculated as an average slope during Stage 2. K-7 showed the gentlest slope, where the change in AE was lower with time compared to the other profiles. This behavior is related to the microscale development of the unsaturated layer, which was explained in Hussary et al. (2022b). In the same study, a strong inverse relationship between ΔAE and the receding vaporization plane with time (ΔL) during Stage 2 was found. The vaporization plane represents the bottom boundary of the air-dry layer and reflects the diffusion distance. Assuming that the water diffusion rate through the air-dry layer depends on the pore structure, ΔAE was plotted against the I_{PSD}, as shown in Figure 6. The results show a strong inverse relationship between the I_{PSD} and ΔAE. Therefore, soil profiles with bigger I_{PSD} have a slower reduction in AE, delineating gentler slopes during Stage 2. Based on that, it can be concluded that for homogeneous sandy soil profiles under steady atmospheric demand, the change in the actual evaporation rate during Stage 2 is a function of the I_{PSD}, which reflects the efficiency of the soil profile in supplying water to the air layer adjacent to the soil surface.

4. CONCLUSIONS

This study investigated the direct relation between the I_{PSD} and the change in the actual evaporation rate during Stage 2. Based on the results, it was concluded that the newly proposed index is reliable for reflecting the efficiency of the soil in supplying water to the surface during the falling rate stage. This confirms the ability to consider the I_{PSD} as a fundamental parameter in determining the actual evaporation rates from homogenous sandy soil profiles.

Table 1: Soil columns' physical properties

		K-7	K-6	K-5	K-4
Specific gravity	Gs	2.65	2.64	2.65	2.65
Void ratio	e	0.78	0.75	0.76	0.75
Dry density	ρ_d (g/cm^3)	1.48	1.50	1.50	1.50
Effective size	D_{10} (mm)	0.10	0.20	0.31	0.47
Pore Size Distribution Index	I_{PSD} (10^{-4}/μm)	14.5	7.87	1.29	1.82

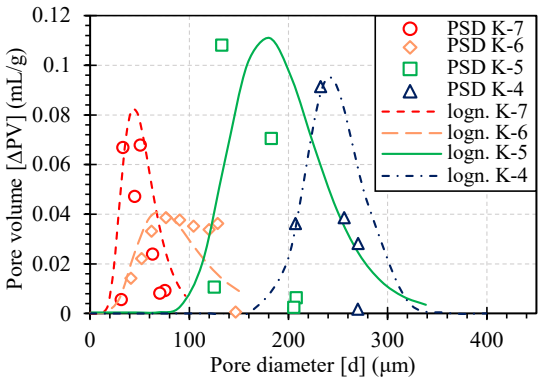

Figure 4: Pore size distribution curves

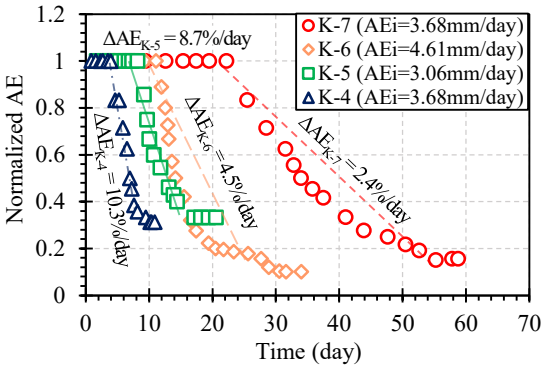

Figure 5: Normalized actual evaporation curves

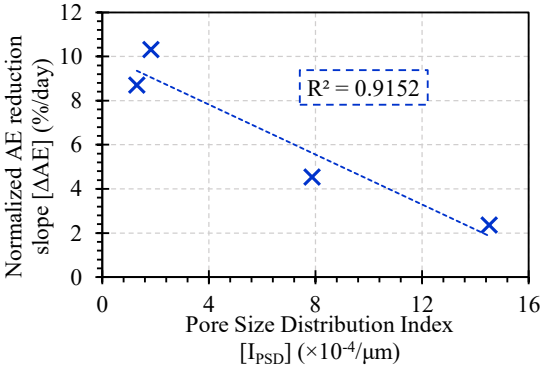

Figure 6: Relationship between ΔAE during Stage 2 and the I_{PSD}

REFERENCES

Alowaisy, A., Yasufuku, N., Ishikura, R., Hatakeyama, M., and Kyono, S.: Continuous pressurization method for a rapid determination of the soil water characteristics curve for remolded and undisturbed cohesionless soils, Soils and Foundations, 60-3, 2020, pp. 634–647.
Hussary, J., Alowaisy, A., Yasufuku, N., Ishikura, R., and Abdelhadi, M.: Pore structure and falling rate stage of evaporation in homogeneous sandy soil profiles, Soils and Foundations, 62-2, 2022a, 101108.
Hussary, J., Alowaisy, A., Yasufuku, N., and Ishikura, R.: Unsaturated layer dynamics during the evaporation stages in homogeneous sandy soil profiles, 土木学会西部支部研究発表会, Japan, 2022b, pp. 377-378.